16.3 INTERCOMPARISON BETWEEN DIFFERENT PBL OPTIONS IN WRF MODEL: MODIFICATION OF TWO PBL SCHEMES FOR STABLE CONDITIONS

R. Dimitrova[*1,2] , Z. Silver[1], H.J.S. Fernando[1], L. Leo[1], S. Di Sabatino[1,3], C. Hocut[1,5], T. Zsedrovits[1,4]
[1]University of Notre Dame, Civil and Environmental Engineering and Earth Sciences
[2]National Institute of Geophysics, Geodesy and Geography, Bulgarian Academy of Sciences
[3]Salento University, Micrometeorology Laboratory
[4]Pazmany Peter Catholic University, Faculty of Information Technology and Bionics
[5]U.S. Army Research Laboratory

1. INTRODUCTION

During the last decade, the scientific community has placed an enormous effort into improving high-resolution meso-scale numerical modeling. The importance of parameterization has been well recognized and a lot of work has been done. However, efforts on improved boundary layer parameterization in meso-scale numerical models are continuing because of the difficulties of representing small-scale processes, especially during the nocturnal and transition periods. Turbulence parameterization continues to be a challenge. Interactions of various scales and associated fluxes are problematic to represent in the models. Boundary layer and surface exchange parameterizations are typically based on knowledge of atmospheric turbulence from relatively homogeneous, flat terrain and under optimal circumstances, i.e. near-steady-state conditions with neutral or weakly stable or unstable stratification. These conditions are not present in complex topography. There may be very heterogeneous land-use patterns, mountains with narrow valleys and steep slopes or at least hills, all of which lead to horizontally inhomogeneous Planetary Boundary Layers (PBL) (Rotachand & Zardi 2007).

One of the goals of the on-going Mountain Terrain Atmospheric Modeling and Observations Program (www.nd.edu/~dynamics/materhorn) MATERHORN is to identify and understand the deficiencies – structural, physics and dynamics in meso-scale models and improve model predictions. High-resolution runs of the Advanced Research version of the Weather Research and Forecasting (WRF) model were completed to test the abilities of the code for mountain terrain numerical modeling. Data from two MATERHORN field campaigns were used. The capabilities and limitations of different PBL options available in the WRF model was investigated and compared against meteorological data collected during the two field campaigns. Modeling outcomes from six PBL schemes: YSU (YonSei University), MRF (Medium Range Forecast), ACM2 (Asymmetric Convective Model), MYJ (Mellor – Yamada - Janjic), BouLac (Bougeault - LaCarrere) and QNSE (Quasi-Normal Scale Elimination), were compared with a large number of observations. A new turbulent parameterization for the stable lower atmosphere proposed by Monti et al. (2002) has been implemented in two PBL schemes - YSU and MRF. A unique aspect of this parameterization is the stability dependence of the turbulent Prandtl number that allows momentum to be transported by internal waves, while heat is diffused by turbulent eddies, which are suppressed due to stable stratification; thus the momentum diffuses faster than heat.

* Corresponding author: Reneta Dimitrova, University of Notre Dame, Civil and Environmental Engineering and Earth Sciences, Notre Dame, Indiana, 46556 USA,
E-mail: Reneta.Dimitrova@nd.edu

2. MODEL SET UP

The Advanced Research version of the Weather Research and Forecasting model (ARW-WRFv3.4.1., release on August 16, 2012) was employed in this study. The ARW-WRF model is a state-of-the-art atmospheric meso-scale numerical weather prediction system, suitable for use in a broad range of applications (http://www.mmm.ucar.edu/wrf/users).

2.1 Modeling domains

The modeling domain was based on a Lambert Projection centered at 113^{O}W, 40^{O}N (located in Utah). Four two-way nested domains of 64, 16, 4 and 1km grids were used. The geographical framework within this work is shown (Fig.1a) together with the locations of instruments that provided data used for the model evaluation (Fig.1b). The experimental domain was the Dugway Proving Ground (DPG). DPG is a U.S. Army facility located approximately 85 miles (140km) southwest of Salt Lake City, Utah. It covers 798,214 acres of the Great Salt Lake Desert, and is surrounded on three sides by mountain ranges. The outcomes presented in the paper are only from the innermost domain with 1x1 km grids which includes Granite Peak (Fig.1b).

The vertical grid was setup with 48 terrain following (eta) levels. More points were employed in the lowest part of the PBL (27 levels in the lowest 1000m) to increase the vertical resolution in the stable boundary layer (SBL). In the two-way nested simulations, multiple domains at different grid resolutions were run simultaneously while communicating with each other - the coarser domain provides boundary values for the nest, and the nest feeds its calculation back to the coarser domain. The initial and boundary conditions for the ARW-WRF are based on the NCEP Final Operational Model Global Tropospheric Analyses every six hours (http://rda.ucar.edu/datasets/ds083.2/). This product comes from the Global Data Assimilation System, which continuously collects observational data from the Global Telecommunications System.

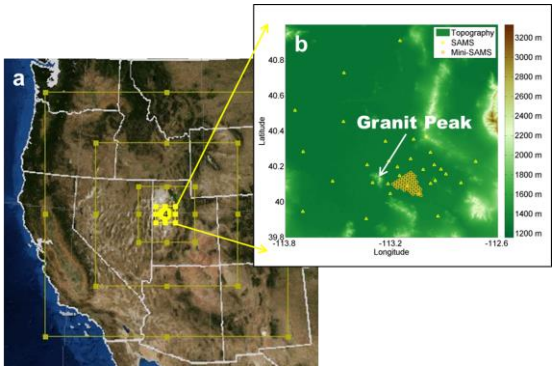

Figure.1 Model domains for the numerical simulations (a), the inner domain (1km grid) with the location of instruments used for model evaluation (b)

In 2012, the land-cover and terrain elevation dataset was updated based on the newer 33-category National Land Cover Database (NLCD) dataset (Fry et al., 2011). The new land-cover increased the area defined as playa. The soil-texture class is defined by a 16-category United States Geological Survey (USGS) dataset, which is also modified to include playa, white sand, and lava soil texture classes. The updated database was used together with a new parameterization of soil thermal conductivity in the Noah land-surface model for silt loam and sandy loam soils proposed by Massey et al. (2013) that provide significant nocturnal temperature bias reduction.

2.2 Modeling periods

This case study covers six Intensive Operational Periods (IOP) with quiescent large-scale conditions (defined as a period where the wind speed is less than 5 m/s at 700 mb). The main focus was to isolate local land-atmosphere processes under stable conditions. The simulated IOPs from both MATERHORN field campaigns are listed in Table 1.

In order to perform a proper model experiment, sufficient spin-up time (12 hours or more, depending on the starting time for the different IOPs) was taken into account.

IOP	Run Date and Times (MDT)
Fall campaign	
1	9/28/2012 14:00 - 9/29/2012 14:00
2	10/1/2012 14:00 - 10/2/2012 14:00
6	10/14/2012 2:00 - 10/15/2012 2:00
8	10/18/2012 5:00 - 10/19/2012 12:00
Spring campaign	
4	5/11/2013 14:00- 5/12/2013 14:00
7	5/20/2013 17:15 - 5/21/2013 14:00

Table 1. Periods for numerical simulations

2.3 Physical options

The physics packages include: a sophisticated microphysics scheme that has ice, snow and graupel processes (Lin et al. 1983), the Rapid Radiative Transfer Model (RRTM) longwave radiation parameterization (Mlawer et al. 1997), Dudhia shortwave radiation parameterization (Dudhia 1989), Noah land surface model (Chen & Dudhia 2001), and explicit sixth-order numerical diffusion (Knievel et al. 2007). Most of the available planetary boundary layer (PBL) schemes in ARW-WRF version 3.4.1 were used and compared. These are: Yonsei University - YSU (Hong et al. 2006), Medium Range Forecast - MRF (Hong & Pan 1996), Asymmetric Convective Model - ACM2 (Pleim J. E. 2007a, b), Mellor-Yamada-Janjic - MYJ (Janjic 1990, 1994), Bougeault and Lacarrere - BouLac (Bougeault & Lacarrere 1989), and Quasi-Normal Scale Elimination - QNSE (Sukoriansky et al. 2005).

Two of the PBL schemes (YSU and MRF) are non-local first order schemes and the eddy diffusivity of heat, momentum and moisture use profiles returned to the friction velocity and PBL depth. The PBL depth is estimated using the critical bulk Richardson number method. To allow for non-local vertical fluxes, a non-local term is added in the turbulence diffusion equations for prognostic variables. The major difference between MRF and YSU (extended MRF scheme) is the inclusion of an explicit treatment of entrainment processes at the top of the PBL.

The other first-order PBL scheme selected for this study was the Asymmetric Convective Model, version 2 (ACM2). This PBL scheme is a combination of the local and non-local mixing approach (explicit non-local upward mixing and local downward mixing). ACM2 shuts off nonlocal transport and uses local closure for stable and neutral conditions.

The remaining PBL schemes used in this study (MYJ, BouLag and QNSE) are turbulent kinetic energy (TKE) closure schemes. In all the above-mentioned schemes, only local transport is allowed and the diffusivity can be expressed as multiplication of the mixing length scale, root square of TKE and proportional coefficient. They differ in the definitions of the mixing length and the proportionality coefficient.

The surface-layer (SL) schemes, which are used together with the PBL schemes, are listed in Table 2. The simulations with the YSU and MRF PBL schemes were performed with the MM5 scheme (Zhang & Anthes 1982; Grell et al. 1994). For the MYJ and BouLac, the Janjic Eta Monin-Obukhov surface-layer scheme (Janjic 1990, 1994) was used. The last two, ACM2 and QNSE schemes, were coupled with the surface-layer schemes that were specially developed for them: Pleim-Xiu (PX) (Pleim 2006) and Quasi-Normal Scale Elimination (Sukoriansky 2005). All four surface-layer schemes are based on the Monin–Obukhov similarity theory, but with differences in their specific treatments of stability functions and the various empirical parameters embedded in the different parameterizations.

Type PBL scheme	PBL scheme	SL Scheme
First order closure	MRF/YSU ACM2	MM5 PX
TKE closure	MYJ/BouLag QNSE	Eta QNSE

Table 2. Schemes use in the PBL experiment

3. OBSERVATIONS

The Granite Mountain Atmospheric Sciences Testbed (GMAST) facility of DPG has several different networks of permanently fixed weather stations. One of these networks is the Surface Atmospheric Measurement (SAMS) network. This system consists of thirty-one towers. A second closely related system is the Mini-SAMS network with fifty-one towers. The two systems both record horizontal wind speed, wind direction, and temperature at 2 and 10 meters above the surface. Both the SAMS and the Mini-SAMS measure additional atmospheric conditions, however the latter contains fewer measurement probes. These measurement networks were used to determine how the WRF model performed over a large area for the GMAST facility. The inner domain of the WRF model simulations contained all Mini-SAMS towers. The model was statistically correlated with each individual station. However, the SAMS network is spread out over a greater area. Only eighteen stations were used in this work.

4. MODELING RESULTS AND DISCUSSION

Numerical simulations were performed for all IOP cases using all six PBL schemes. Different statistical measures (see the Appendix) were calculated for the nighttime period (7pm until 6am) using data from the network described in paragraph 3.

4.1 PBL experiment

Averaged values of temperature, wind speed and wind direction, along with the corresponding standard deviation for different PBL schemes, are shown in Table 3. The wind speed and direction were extracted from the WRF grid cells that corresponded with each individual SAMS and Mini-SAMS tower. Using the log-law wind profile, the u and v wind components were calculated at 10 meters. The vertical temperature profile was extracted for each tower location and the temperature was interpolated at 2 meters. The statistics were calculated for all quiescent IOPs. This was accomplished by matching up each half-hour output extracted from the model at a specific grid cell to the corresponding half-hour measured value at the tower corresponding to that grid cell.

	Temperature		Wind speed		Wind direction	
	Av	SD	Av	SD	Av	SD
Obs	***11.09***	***7.21***	***2.65***	***1.27***	***141.78***	***70.01***
YSU	14.36	4.38	2.96	1.61	154.68	78.26
MRF	14.63	4.20	3.12	1.82	155.37	78.91
ACM2	13.89	4.34	3.19	1.41	157.53	75.46
MYJ	13.93	4.28	2.99	1.48	156.87	75.92
BouLag	14.50	4.06	2.94	1.45	159.02	79.11
QNSE	**12.73**	4.45	**2.78**	1.14	**149.74**	67.70

Table 3. Averaged values (Av) and standard deviation (SD) for temperature (2m), wind speed (10m) and wind direction (10m) compared to observations (Obs)

All of the PBL schemes over-predicted the average temperature with about 2-3 degrees and provided close results to the average value for the wind speed (0.5m/s or less difference) with some variation in the main southeast wind direction (the variance is between 8-17 degrees). Overall, the Quasi-Normal Scale Elimination (QNSE) performed better, considering both temperature and wind.

Different statistical measures are listed in Table 4. It is difficult to make a clear conclusion about a preferred PBL scheme based only on these statistics. These statistics are related only to the near surface model performance.

	Temperature		Wind speed		Wind direction	
	RMSE	IA	RMSE	IA	RMSE	IA
YSU	6.51	0.69	1.96	0.45	97.46	0.51
MRF	6.64	0.67	2.10	0.46	98.99	0.50
ACM2	6.28	0.70	1.85	0.46	94.70	0.53
MYJ	6.29	0.69	1.84	0.47	94.08	0.53
BouLag	6.63	0.66	1.80	**0.48**	93.92	**0.56**
QNSE	**5.77**	**0.73**	**1.57**	**0.48**	**89.65**	0.52

Table 4. Summary of statistical measures: Root Mean Square Error (RMSE) and Index of Agreement (IA)

The lowest RMSE for all variables had the QNSE scheme. This scheme also had the best IA for the temperature 0.73 (complete agreement if IA=1). For the wind all schemes had similar IA values in the range of 0.45 - 0.48 for the speed and 0.50 - 0.56 for the direction. The BouLag scheme performed the best for the wind direction.

Comparison of mean biases and mean absolute errors for different PBL schemes are shown in Fig.2. All schemes produced a warm bias of temperature between 1.5 - 3.5 degrees and slightly over-predicted the wind speed (less than 0.5 m/s) for nocturnal stable conditions. The QNSE shows the best performance for near surface values.

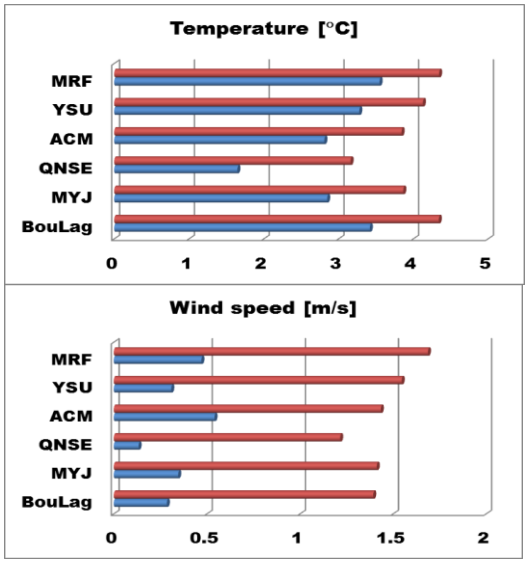

Figure 2. Mean bias (blue) and mean absolute errors (red) for different PBL schemes

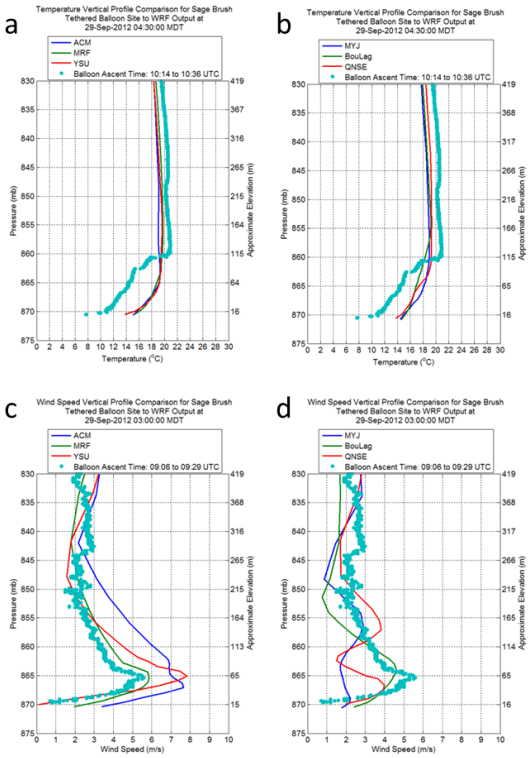

Figure 3. Vertical profiles of different PBL schemes for the temperature (a, b) and the wind speed (c, d), compared with observations.

Comparison of vertical profiles for temperature and wind speed are shown in Figure 3 separately for the first-order (3a, c) and TKE closure (3b, d) schemes at the Sagebrush site (balloon data) for IOP1. All schemes provided similar results for temperature (Fig. 3a, 3b), and were not able to capture the depth of the stable layer and the steep temperature gradient of the early morning. All first-order PBL schemes (Fig. 3c) over-predicted the lower-jet wind speed under strong stable conditions before sunrise, with the best performance shown by ACM2. All TKE closure schemes (Fig. 3d) under-predicted the maximum speed of the nocturnal low-level jet and showed disagreement with observations from above the jet layer.

4.2 Modification of MRF and YSU schemes for stable conditions

The existing parameterizations cannot accurately capture the depth of the stable BL, the low-level jet and the nocturnal near surface temperature because of poor representation of turbulent flux parameterizations, especially for mountain terrain. All PBL schemes used had the same disadvantages: over-predicting the minimum temperature inside the "valley cold pool" and they cannot accurately capture the maximum velocity of the low-level jet. Several studies have shown that local closure schemes perform better under stable conditions, but they demonstrate worse performance for the convective BL (Hu et al. 2010; Shin & Hong 2011; Garcıa-Dıez 2011; LeMone et al. 2013). The MRF and YSU (extended MRF) schemes are simpler, suited for numerical weather prediction, computationally inexpensive and well evaluated for different conditions and areas. The modification made for both schemes combines the advantages of the original scheme with the use of local closure for stable conditions.

Both MRF and YSU schemes use identical profile functions for momentum and heat for stable conditions, leading to a constant turbulent Prandtl number (Pr_t). The experimental data of Strang & Fernando (2001) and Monti et al. (2002) show that both momentum K_m and heat K_h diffusivities are stability (i.e. gradient Richardson Number Ri_g) dependent. Monti et al. (2002) suggested a new parameterization for eddy diffusivities under stable conditions. An advantage of this parameterization is the implementation of a stability varying Pr_t that allows momentum to be transported from a specific region by the internal waves, while heat is diffused by turbulent eddies, which are suppressed due to stable stratification. A normalized parameterizations based on the variance of the vertical velocity σ_w and the shear length scale $\sigma_w \left| d\vec{V}/dz \right|^{-1}$ (Fernando 2003) were proposed, were $\vec{V}$ is the velocity vector.

$$K_m = 0.34 Ri_g^{-0.02} \sigma_w^2 \left| d\vec{V}/dz \right|^{-1}$$

$$K_h = 0.08 Ri_g^{-0.49} \sigma_w^2 \left| d\vec{V}/dz \right|^{-1}$$

Lee et al. (2006) combined these formulae with the empirical formula of Stull (1988) to calculate the vertical velocity variance:

$$\sigma_w^2 = \overline{w'^2} = 2.5 u_*^2 \left[1 - (z/h)^{0.6} \right]$$

were h is the height of the mixed layer, $u_* = \left(-\overline{u'w'} \right)^{1/2}$ is the surface friction velocity scale from the similarity theory. Lee et al. (2006) implemented this new parameterization in the MRF scheme of

MM5v3.7 (Grell et al. 1994) and noted improved performance.

In this work, the same parameterization has been implemented in both MRF and YSU schemes of ARW-WRFv3.4.1 and the model results were compared with results from the original schemes.

One example of the temperature bias (at 2 m) calculated using MRF original (Fig. 4a) and modified (Fig. 4b) PBL schemes are shown for October 19, 2012, at 5 am MDT. The modified model reduces the warm bias by about 2 degrees inside the valley under the stable conditions.

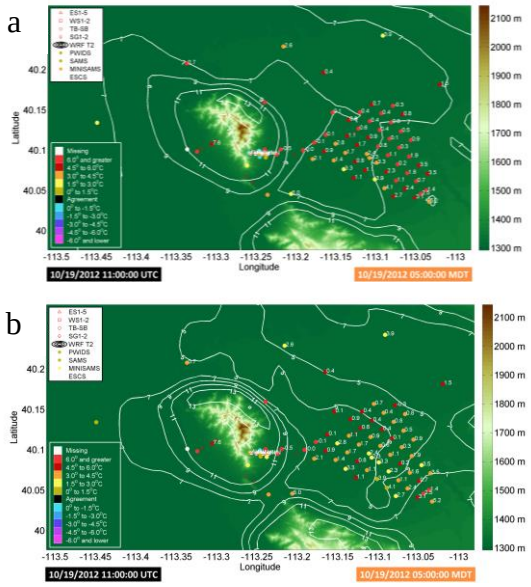

Figure 4. Temperature bias for MRF original (a) and MRF modified (b) for October 19, 2012, 5am MDT

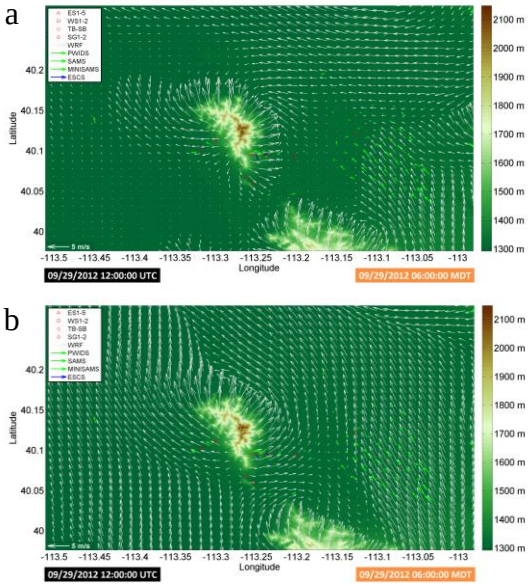

Figure 5. Velocity vectors for YSU original (a) and YSU modified (b) for September 29, 2012, 6am MDT

An example of wind velocity vectors are shown (at 10m) for both the YSU original (Fig.5a) and the modified (Fig.5b) PBL schemes for September 29, 2012, 6 am MDT. The modified version performs better inside the valley. The model captures different flows well - downslope, valley and gap. The gap flow propagates inside the valley suppressing the valley and downslope flows and developing vertical structures in front of the east slope. The collision area is well displayed, in broad agreement with observations.

Vertical profiles of temperature (Fig. 6a) and wind speed (Fig. 6b) were compared with the balloon data at the Sagebrush site. Two different surface layer schemes were used with the modified PBL schemes. The first one, called MM5, is based on the fifth-generation Pennsylvania State University – National Center for Atmospheric Research Mesoscale Model (Zhang & Anthes 1982, Grell et al. 1994), the second one is revised MM5 scheme (Jimenez et al. 2012). Both are based on the Monin-Obukhov theory and the difference lies in the similarity functions employed. The revised scheme provides more suitable similarity functions to simulate the surface layer under strong stable conditions and it reduces or suppresses limits that are imposed on certain variables in order to avoid undesirable effects (lower limit for u*=0.1).

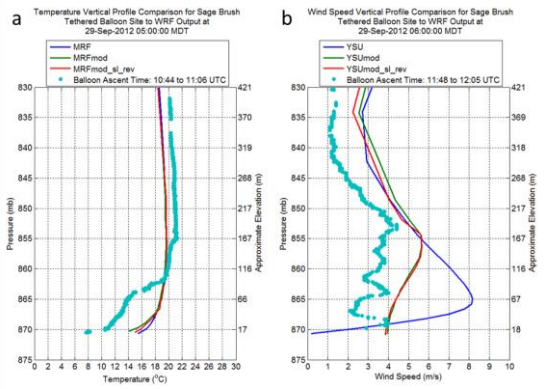

Figure 6. Vertical profiles of temperature based on MRF (a) and wind speed based on YSU (b) schemes compared with observations. Blue line indicate the original PBL schemes, green - modified model with MM5 original surface layer, red line – modified model with MM5 revised surface layer

The MRF modified model performs better with the original MM5, YSU modified model – with the revised one. The difference in comparing the original and modified PBL schemes mainly occurs inside the stable layer. New parameterization reduces the temperature about 1.5 - 2 degrees, but the warm bias inside the stable layer of the "valley cold pool" remains. The most significant improvement can be seen in the velocity profile.

The maximum of the lower level jet is moved to the top of the stable layer, in agreement with observations. The model still over-predicts velocity magnitude by about 1m/s, and it could not capture the layered structure within the stable layer.

4. CONCLUSIONS

This work was conducted under the MATERHORN Program to understand the ability of WRF model to predict near surface flow and temperature for stable conditions in mountain terrain. Six different PBL schemes were evaluated against observations, and all of them over-predict the minimum temperature inside the "valley cold pool" and could not capture the low-level jet and vertical layering in the stratified layer. The advantages and disadvantages of each scheme were identified for this case, focusing on the prediction of near-surface and PBL properties. For our case, the QNSE scheme was the best performer of near surface temperature (2m) and wind (10m) during SPBL.

The preliminary results show better performance of the modified MRF scheme, which slightly improved the minimum temperature, and the modified YSU scheme, which reduced the maximum velocity of the low-level jet. The surface layer parameterizations only contributed to near-surface variability, and the shapes of profiles are determined by the PBL mixing algorithms. Further evaluation and testing of modified PBL and existing surface layer schemes is necessary.

5. ACNOWLEGEMENTS

This research was funded by Office of Naval Research Award # N00014-11-1-0709, Mountain Terrain Atmospheric Modeling and Observations (MATERHORN) Program with additional support from The European Union and the State of Hungary in the framework of TÁMOP-4.2.1.B-11/2/KMR-2011-0002 Instrument.

This research was supported in part by the Notre Dame's Center for Research Computing through computational and storage resources. We specifically acknowledge the assistance of Dodi Heryadi.

We specifically thank Jeffrey Massey from the University of Utah for the updated land cover and soil data provided.

6. REFERENCES

Bougeault, P., P. Lacarrere, 1989: Parameterization of orography-Induced turbulence in a mesobeta–scale model. *Mon Wea Rev,* 117 (8), 1872–1890

Chen, F., J. Dudhia, 2001: Coupling an advanced land surface-hydrology model with the Penn State-NCAR MM5 modeling system. Part I: Model implementation and sensitivity. *Mon Wea Rev*, 129, 569–585

Dudhia, J., 1989: Numerical study of convection observed during the winter monsoon experiment using a mesoscale two-dimensional model. *J Atmos Sci*, 46, 3077–3107

Fernando, H. J. S., 2003: Turbulence patches in a stratified shear flow. *Phys Fluids*, 15 (10), 3164-3169

Fry, J., G., Xian, S. Jin, J. Dewitz, C. Homer, L. Yang, C. Barnes, N. Herold, J. Wickham, 2011: Completion of the 2006 national land cover database for the conterminous United States, *PE&RS*, 77, 858-864

Grell, G. A., J. Dudhia, D.R. Stauffer, 1994: A description of the fifth-generation Penn State/NCAR mesoscale model (MM5), *NCAR Technical Note*, NCAR/TN-398+STR

Garcıa-Dıez M., J. Fernandez, L. Fita, C. Yague, 2011: Seasonal dependence of WRF model biases and sensitivity to PBL schemes over Europe. *Q J R Meteorol Soc*, 00, 2–21

Hong, S. Y., H. L. Pan, 1996: Nonlocal boundary layer vertical diffusion in a Medium-Range Forecast Model. *Mon Wea Rev*, 124 (10), 2322–2339

Hong, S., Y. Noh, J. Dudhia, 2006: A new vertical diffusion package with an explicit treatment of entrainment processes. *Mon Wea Rev*, 134 (9), 2318–2341

Hu, X. M., J. W. Nielsen-Gammon, F. Zhang, 2010: Evaluation of three planetary boundary layer schemes in the WRF model. *J Appl Meteorol Clim*, 49, 1831-1844

Janjic, Z., 1990: The step-mountain coordinate: physics package. *Mon Weather Rev*, 118, 1429–1443

Janjic, Z., 1994: The step-mountain eta coordinate model: further development of the convection, viscous sublayer, and turbulence closure schemes. *Mon Wea Rev*, 122, 927-945

Jiménez, P. A., J. Dudhia, 2012: Improving the representation of resolved and unresolved topographic effects on surface wind in the wrf model. *J Appl Meteorol Clim*, 51 (2), 300–316

Knievel, J. C., G. H. Bryan, J. P. Hacker, 2007: Explicit numerical diffusion in the WRF Model. *Mon. Wea. Rev*., 135, 3808–3824

Lee, S.M., W. Giori, M. Princevac, H. J. S. Fernando, 2006: Implementation of a stable PBL turbulence parameterization for the mesoscale model MM5: nocturnal flow in complex terrain. *Boundary-Layer Meteorol*, 119, 109-134

LeMone, M. A., M. Tewari, F. Chen, J. Dudhia, 2013: Objectively Determined Fair-Weather CBL Depths in the ARW-WRF Model and Their Comparison to CASES-97 Observations. *Mon Wea Rev*, 141 (1), 30-54

Lin, Y.-L., R. D. Farley, and H. D. Orville, 1983: Bulk parameterization of the snow field in a cloud model. *J. Climate Appl. Meteor*., 22, 1065–1092.

Massey, J., W. J. Steenburgh, S. W. Hoch, J. C. Knievel, 2013: Sensitivity of near-srface temperature forecasts to soil properties over a sparsely vegetated dryland region. *J Appl Meteorol Clim*

Mlawer, E. J., S. J. Taubman, P. D. Brown, M. J. Iacono, S. A. Clough, 1997: Radiative transfer

for inhomogeneous atmospheres: RRTM, a validated correlated-k model for the longwave. *J Geophys Res: Atmos,* 102 (14), 16,663–16,682

Monti, P., H. J. S. Fernando, M. Princevac, W. C. Chan, T. A. Kowalewski, E. R. Pardyjak, 2002: Observations of flow and turbulence in the nocturnal boundary layer over a slope. *J Atmos Sci*, 59, 2513–2534

Pleim, J. E., 2006: A simple, efficient solution of flux-profile relationships in the atmospheric surface layer. *J Appl Meteorol Clim*, 45 (2), 341–347

Pleim, J. E., 2007a: A combined local and nonlocal closure model for the atmospheric boundary layer. Part I: Model description and testing. *J Appl Meteorol Clim*, 46 (9), 1383–1395

Pleim, J. E., 2007b: A combined local and nonlocal closure model for the atmospheric boundary layer. Part II: Application and evaluation in a mesoscale meteorological model. *J Appl Meteorol Clim*, 46 (9), 1396–1409

Rotach, M.,W., D. Zardi, 2007: On the boundary layer structure over highly complex terrain: key findings from MAP, *Quarterly J Roy Meteorol Soc*,133, 937–948

Shin, H. H., · S. Y. Hong, 2011: Intercomparison of Planetary Boundary-Layer parametrizations in the WRF model for a single day from CASES-99. *Boundary-Layer Meteorol*, 139, 261–281

Strang, E. J., H. J. S. Fernando, 2001: Vertical mixing and transports through a stratified shear layer, J Phys Oceanogr, 31, 2026-2048

Stull, R. B., 1988: An introduction to boundary layer meteorology. *Kluwer Academic Publishers, Dordrecht*, 666 pp.

Sukoriansky, S., B. Galperin, V. Perov, 2005: Application of a new spectral theory of stably stratified turbulence to the atmospheric boundary layer over sea ice. *Boundary-Layer Meteorol*, 117 (2), 231–257

Zhang, D., R. A. Anthes, 1982: A high-resolution model of the planetary boundary layer—sensitivity tests and comparison with SESAME-79 data. *J Appl Meteorol*, 21, 1594–1609

Appendix

The following indicators were used for performance evaluation. Here **P** is the predicted value, **O** the observed value, and $\overline{\mathbf{P}}$ and $\overline{\mathbf{O}}$ the mean values.

$$\mathbf{MAE}=\frac{1}{\mathbf{N}}\sum_{i=1}^{N}|\mathbf{P}_i-\mathbf{O}_i|$$ (Mean Absolute Error)

$$\mathbf{MB}=\frac{1}{\mathbf{N}}\sum_{i=1}^{N}(\mathbf{P}_i-\mathbf{O}_i)$$ (Mean Bias)

$$\mathbf{RMSE}=\sqrt{\frac{\sum_{i=1}^{N}(\mathbf{P}_i-\mathbf{O}_i)}{\mathbf{N}}}$$ (Root Mean Square Error)

$$\mathbf{IA}=1-\frac{\sum_{i=1}^{N}\left(\mathbf{P}_i-\mathbf{O}_i\right)^2}{\sum_{i=1}^{N}\left(\left|\mathbf{P}_i-\overline{\mathbf{O}}_i\right|+\left|\mathbf{O}_i-\overline{\mathbf{O}}_i\right|\right)^2}$$ (IA Index of Agreement)